Scientific Research Publishing

Materials Sciences and Applications, 2023, 14, 63-77
https://www.scirp.org/journal/msa
ISSN Online: 2153-1188
ISSN Print: 2153-117X

Characterization of the Natural and Organomodified Clay Soil of Moukosso (Republic of Congo) by Dimethylsulfoxide: Application to the Adsorption of Lead (II) in Aqueous Solution

Ottard Arnaud M. R. Ossiby Mwa Ngo[1], Ferland Ngoro-Elenga[1,2,3*], Erman E. Nzaba Madila[4], Zita F. Diamouangana Mpissi[1,5], Exaucé R. Kinzonzi Ngongot[1], Joseph Marie Moutou[1,5]

[1]Laboratoire de Chimie Minérale et Appliquée, Faculté des Sciences et Techniques, Université Marien Ngouabi, Brazzaville, Congo
[2]Faculté des Sciences et Techniques, Université Marien Ngouabi, Brazzaville, Congo
[3]Centre de Recherches Géologiques et Minières, Brazzaville, Congo
[4]Institut de Recherche sur l'Hydrogène, Université du Québec à Trois-Rivières, Québec, Canada
[5]Ecole Normale Supérieure, Université Marien Ngouabi, Brazzaville, Congo
Email: *ferland.ngoro-elenga@umng.cg, *fngoroelenga@gmail.com

How to cite this paper: Ossiby Mwa Ngo, O.A.M.R., Ngoro-Elenga, F., Nzaba Madila, E.E., Diamouangana Mpissi, Z.F., Kinzonzi Ngongot, E.R. and Moutou, J.M. (2023) Characterization of the Natural and Organomodified Clay Soil of Moukosso (Republic of Congo) by Dimethylsulfoxide: Application to the Adsorption of Lead (II) in Aqueous Solution. *Materials Sciences and Applications*, **14**, 63-77.
https://doi.org/10.4236/msa.2023.142005

Received: December 2, 2022
Accepted: February 12, 2023
Published: February 15, 2023

Abstract

In this study, the authors characterized the raw clayey soil of Moukosso and modified by dimethylsulfoxide (DMSO) by several analytical methods, namely: X-ray diffraction (XRD), Fourier transform infrared (FTIR) and gravimetric thermal analysis (TGA). The cation exchange capacity (CEC) was also determined. Mineralogical analysis by XRD revealed the presence of muscovite (29.7%), kaolinite (8.9%), anatase (2.4%) and quartz (58.9%). The characterization of the organo-clay by infrared and by thermogravimetric analysis confirmed the intercalation of DMSO by the presence of vibration bands at 1008 cm^{-1} and 1070 cm^{-1} and a strong increase in the loss of mass. The cation exchange capacity of the raw material is 7.4 meq/100g. Rapid adsorption of Pb^{2+} ions was observed between 5 and 15 minutes of stirring time in both cases (raw clay and organomodified clay). The modeling of the isotherms by the models of Langmuir and Freudlich showed that these are of type S with a maximum amount of adsorption of 22.471 mg/g for the fine fraction and 41.493 mg/g for the clay intercalated with DMSO. Langmuir's model best reproduces the experimental data of this study.

Keywords

Clay, Dimethylsulfoxide, Organoclay, Characterization, Adsorption,

Isotherm, Moukosso

1. Introduction

Awareness of the environmental problem in general and waste management, in particular, is now an integral part of the development strategies designed and implemented in every country at both national and sectoral levels [1]. Clay minerals are arguably the most encouraging alternatives to expensive adsorbents. Clays are abundant and widely available materials, exhibiting good chemical and mechanical stability and having unique adsorption and ion exchange properties [2] [3] [4]. Due to their local availability, technical feasibility and cost-effectiveness, studies have been conducted on the use of clay minerals for wastewater treatment applications [5]-[10]. Thanks to their interesting surface properties, clays behave as natural cleaning agents and absorb organic and inorganic contaminants present in water, both by ion exchange and by adsorption. The modification of the surface of clays most often promotes the creation of new materials that can have many practical applications in several fields of materials science. Organic and inorganic pollutant adsorbents, rheology control agents, paints, cosmetics, personal care products, catalysts, soil remediation, electrodes and nano-composite precursors are among examples of the results of modification of clay surfaces [3] [4] [11] [12] [13]. Due to their relatively low production cost and high adsorption capacity, adsorption by organoclays has been used for the removal of organic and inorganic contaminants in waters [14] [15] [16]. As part of the valorization of local materials, we have conducted a study of the Moukosso's clay soil and its application in the adsorption of Pb^{2+} ions. Environmental pollution by heavy metals is a public health problem. Several treatment processes have been developed to remove these metals. Clays, thanks to their nanometric sizes and their sheet structures, offer a large adsorption surface. They are thus used in many pollutant removal processes [17] [18] [19]. It is in this context that we have, after characterization, used the Moukosso's clay soil (raw and chemically modified clay) as an adsorbent to eliminate the Pb^{2+} ions.

2. Methodology

2.1. Location of the Sampling Site

The clay material that is the subject of this study comes from the locality of Moukosso in the department of Bouenza, Republic of Congo. The geographical coordinates of the sampling site are: latitude: 03˚74.963E, longitude: 9˚539.466N. This material was sampled at a depth of 2.5 meters.

2.2. Intercalation of the Clay Fraction by DMSO

The intercalation of DMSO was made in the phyllite fraction extracted from the material. 2.5 g of the fine fraction and 15 mL of the DMSO were mixed in a flask.

The mixture was then refluxed for 12 hours at 150˚C. The solid material obtained was washed several times with isopropanol; then separated by centrifugation. The solid obtained is dried at 60˚C in an oven [20].

2.3. Samples Characterization

1) Determination of cation exchange capacity

The cation exchange capacity of the studied material was determined by the ammonium acetate method [21].

2) Thermogravimetric analysis (TGA)

The thermogravimetric analysis (TGA) was carried out by a Diamond Pyris 6000 device Perkin-Elmer TGA/DTA in the temperature range of 30˚C to 850˚C using aluminum crucibles under N_2 flow at a heating rate of 20˚C/min. The temperature accuracy of the device is ±0.5˚C. Data were processed using Origin software.

3) Fourier Transform Infrared Analysis

The infrared spectroscopy measurements were carried out on a Nicolet iS 10 Smart FT-IR device. The infrared spectrum of the material was realized in the range 4000 - 500 cm^{-1}. Data were processed using Origin software.

4) X-ray diffraction Analysis

The mineralogical analysis by X-ray powder diffraction was carried out on a Panalytical X' Pert Pro MPD type device using the Kα line of copper with a wavelength λ=1.5406 $\mathring{A}$. The data was processed using QualX software.

2.4. Adsorption Test

In order to study the adsorption isotherms, the mass of adsorbent was kept constant and we varied the concentration of the adsorbate. In 50 mL beakers, we introduced 0.05 g of clay and 10 mL of lead chloride solution of concentration in mol/L (0.0002; 0.0003; 0.0005; 0.001; 0.002 and 0.003). The solutions are stirred using a magnetic stirrer for 60 minutes, centrifuged and filtered. After filtration, the solutions were assayed by a UV-visible spectrophotometer at 300 nm. The isotherms are obtained by plotting the adsorbed quantity curve Q_e (mg/g) as a function of the equilibrium concentration C_e (mg/L).

3. Result and Discussion

3.1. Cation Exchange Capacity (CEC)

The cation exchange capacity of this material is 7.4 meq/100g. This value between 3 and 15 could be linked to the presence of kaolinite [22]. The low value of the CEC could explain the absence of smectites in this material [23].

3.2. Thermogravimetric Analysis

Figure 1 and Figure 2 present the TGA curves of raw and intercalated materials from Moukosso.

The thermograms obtained have the same appearance, thus showing a loss of

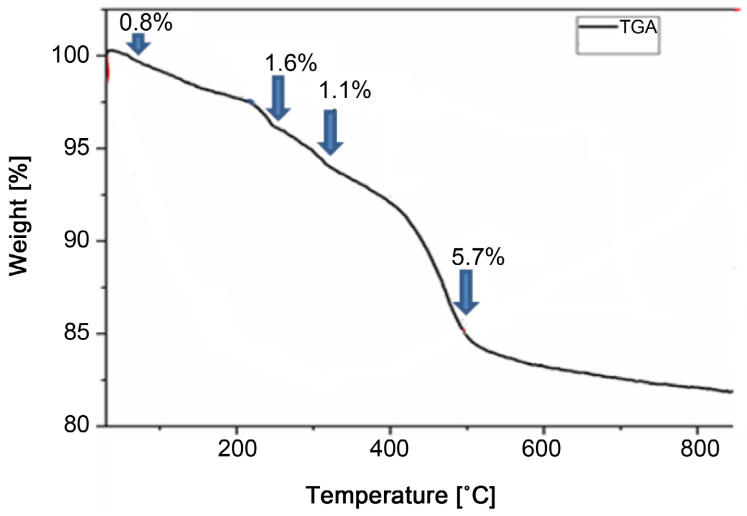

Figure 1. TGA curve of raw clay.

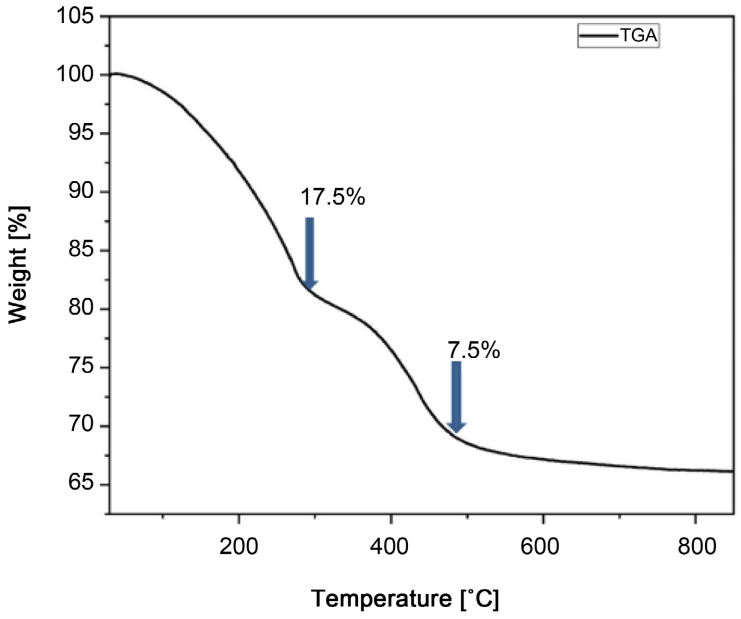

Figure 2. TGA curve of intercaleted clay.

mass through the stepped profile. The one in **Figure 1** shows several differences in level, between

- 0˚C and 100˚C, accompanied by a low mass loss of about 0.8%, would correspond to the departure of surface water from the clay soil [24];
- 200˚C and 250˚C with a mass loss of 1.6% would correspond to the departure of adsorbed water in the interfoliar space [24];
- 280˚C and 300˚C, presents a mass loss of 1.1% which could correspond to the combustion of organic residues and the loss of carbonates [25];
- 450˚C and 600˚C, with a mass loss of 5.7% would correspond to the dehydroxylation of kaolinite [26]. This phenomenon leads to the formation of metakaolinite, an amorphous phase [27].

- 600˚C and 850˚C, the authors observed a progressive loss of mass, a phenomenon which could correspond to the dehydroxylation of muscovite [27].
- On the other hand, that of Figure 2 shows two significant differences in level between:
- 0˚C and 280˚C accompanied by a strong loss of mass of approximately 17.5%, which would correspond to the departure of surface and interfoliar waters and to the decomposition of DMSO. This mass loss is much higher than that obtained with raw clay; which could confirm the success of the intercalation of this clay by DMSO. These results are in agreement with those found in the literature [28].
- 400˚C and 850˚C with a mass loss of 7.5% which could be attributed to the dehydroxylation of kaolinite and muscovite [27].

3.3. Fourier Transform Infrared

Figure 3 and Figure 4 present the infrared spectra of the materials studied.

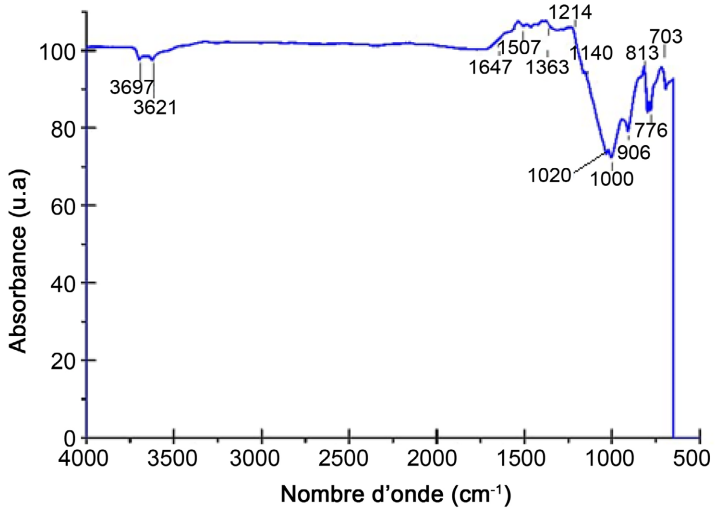

Figure 3. Infrared spectrum of raw material.

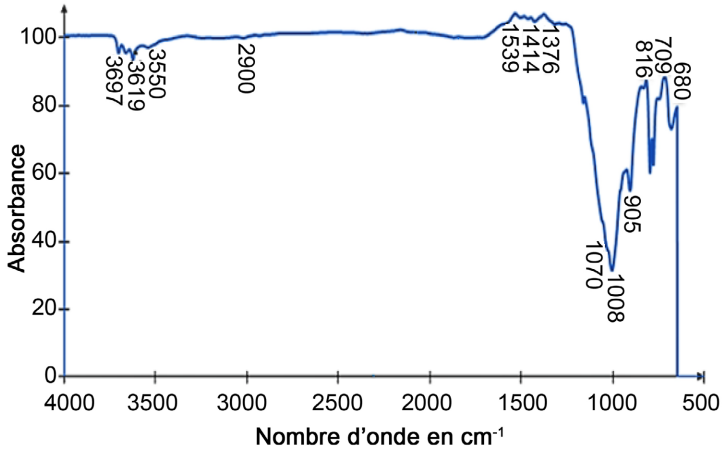

Figure 4. Infrared spectrum of intercaleted material.

For the raw material, we observe the elongation vibration bands at 3697 and 3621 cm^{-1} which could correspond to the OH groups of the kaolinite [29] [30]. The presence of two bands instead of four (3695, 3669, 3650 and 3620 cm^{-1}) would indicate that the kaolinite is poorly crystallized [31]. The band at 3621 cm^{-1} could also be related to the vibration of the OH group of muscovite [32] [33]. The band at 1647 cm^{-1} would correspond to that of hygroscopic water [34]. Bands at 1140 and 1020 cm^{-1} could correspond to Si-O stretching vibrations of kaolinite. The band at 1020 cm^{-1} would also be that of muscovite [32]. The Al-OH deformation vibration characteristic of kaolinite appears at 906 cm^{-1} [35]. The presence of quartz would be indicated by the bands at 813 and 703 cm^{-1}. Compared to the infrared spectrum of the raw material, two bands appear at 3550 cm^{-1} and at 2900 cm^{-1} in the infrared spectrum of the organomodified material. The band at 3550 cm^{-1} would correspond to a new hydroxyl group. However, that at 2900˚C could correspond to the symmetrical stretching mode of CH_2 and CH_3 [36]; it could also be attributed to the valence vibrations of the CH_2 and CH_3 bonds. This confirms that the clay has been intercalated by DMSO, with the presence of the characteristic bands of the S=O bond at 905 cm^{-1} which splits the Al-OH bond of the kaolinite and of the CH3-S bond at 1008 cm^{-1} [36].

3.4. X-Ray Diffraction

Figure 5 shows us the diffractogram of the raw clay of Moukosso.

The qualitative analysis showed the following mineral phases in angular positions (degree): muscovite (8.88; 17.80; 19.86; 20.86; 24.89; 25.52; 26.81; 27, 87; 31.25…), kaolinite $Al_2Si_2O_5(OH)_4$ (12.38; 19.86; 21.32; 24.76; 34.92; 36.94; 39.48…), anatase TiO_2 (25 .32; 36.94; 37.74; 47.96) and quartz SiO_2 (20.86; 26.64; 36.55; 39.47; 40.29; 42.45; 45.8, etc.). These results were also observed by [37] [38]. In contrast, quantitative analysis revealed 58.9% quartz, 29.7% muscovite, 8.9% kaolinite and 2.4% anatase.

3.5. Absorption Spectrum of Lead Chloride

The spectrophotometric dosage of lead chloride made it possible to find the

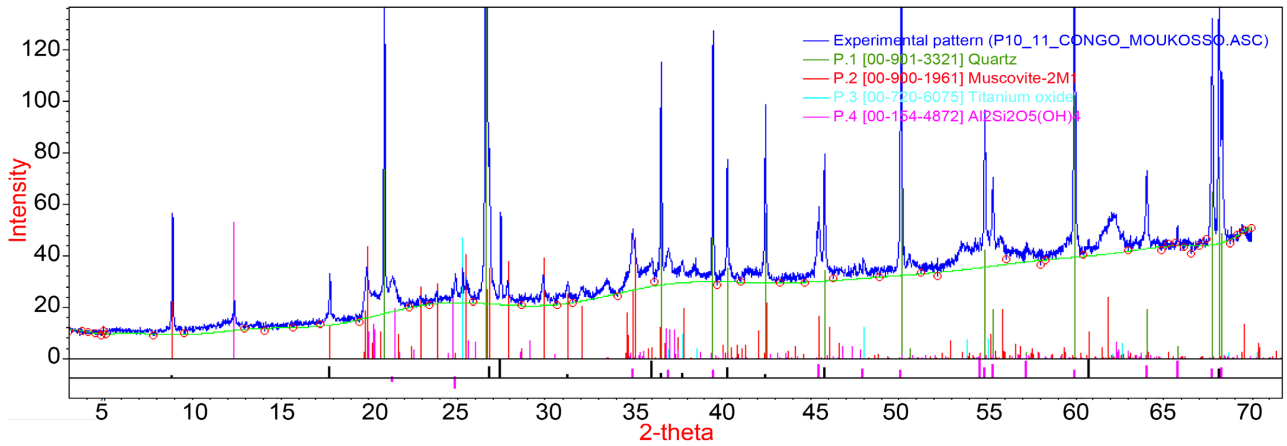

Figure 5. XRD spectrum of raw clay from Moukosso.

wavelength at the maximum of adsorption (λ_{max}) of the Pb^{2+} ions. The results are shown in Figure 6.

Observation of this curve shows that the wavelength at the adsorption maximum is $\lambda_{max} = 300$ nm. This value will be used in the remainder of this study.

3.6. Influence of Stirring Time on the Amountadsorbed

The authors determined the quantity adsorbed by the untreated fine fraction and by the organomodified fine fraction from the formulas:

$$Q_e = \frac{(C_o - C_e)\cdot V}{m} \quad (1)$$

$$C_e = \frac{C_o \times D_{oe}}{D_{oi}} \quad (2)$$

With:

C_o: initial concentration of lead in aqueous solution

C_e: equilibrium concentration (mol/L) of lead in aqueous solution

m: sorbent mass

V: volume of solution

D_{oi}: initial optical density of the solution

D_{oe}: equilibrium optical density of the solution

a) Influence of stirring time on the quantity adsorbed by the fine fraction

Figure 7 shows the evolution of the quantity of Pb^{2+} ions adsorbed by the fine fraction as a function of contact time.

The analysis of this figure shows a rapid adsorption of Pb^{2+} ions by the clay between 5 and 15 minutes of adsorbate-adsorbent contact, followed by a slow increase until equilibrium. This curve shows a balance between 25 and 30 minutes. This equilibrium time could correspond to the maximum efficiency of the adsorption of Pb^{2+} ions on this material. These results are in agreement with those found by [18] [39] [40].

b) Influence of stirring time on the quantityadsorbed by the organomodifiedclay

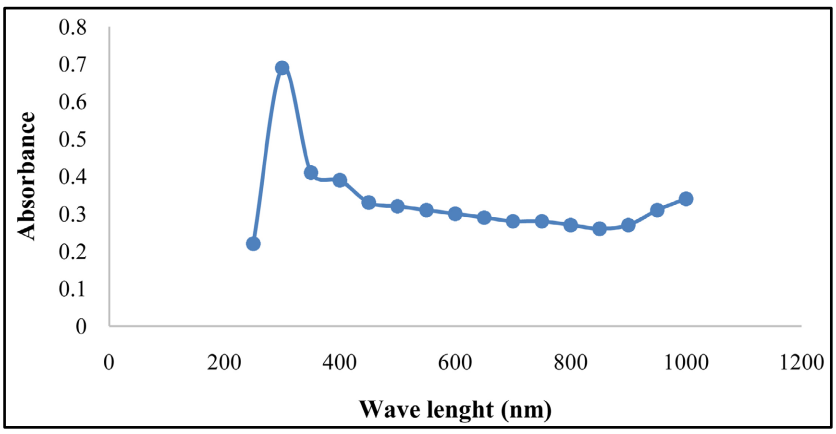

Figure 6. Absorption spectrum of lead chloride.

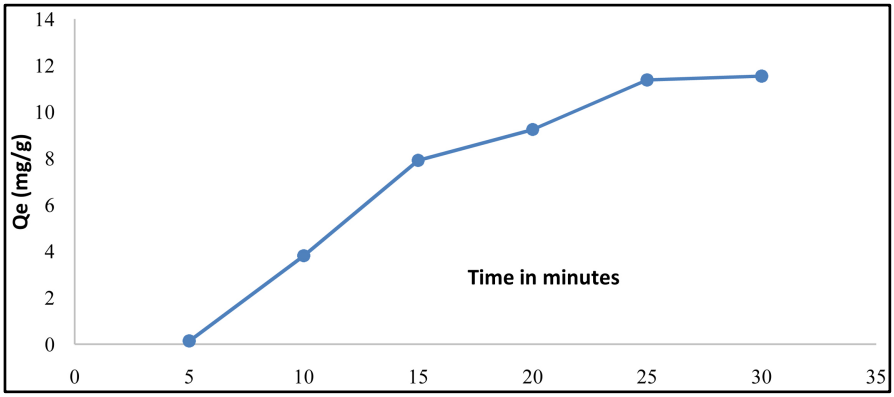

Figure 7. Quantity adsorbed as a function of contact time.

Figure 8 shows the evolution of the adsorbed quantity of Pb^{2+} ions by organomodified clay as a function of stirring time.

There is a strong adsorption of Pb^{2+} ions by the clay between 5 and 15 minutes of agitation, followed by a slow increase between 15 and 30 minutes, which could be related to the saturation of the pores. The clay intercalated by DMSO has a greater adsorption capacity than that of the fine fraction, which would lead to maximum adsorption at the start of contact with the Pb^{2+} ions.

3.7. Adsorption Isotherms of the Fine Fraction and Intercalated Clay

The adsorption isotherms (**Figure 9** and **Figure 10**) are obtained by plotting the curve of the quantity adsorbed at equilibrium of Pb^{2+} ions by the fine fraction and by the organomodified fraction as a function of the equilibrium concentration of Pb^{2+} ions.

The analysis of these figures shows that these adsorption isotherms exhibit the same behavior. These isotherms would be of type S presenting at low concentration, concavities facing upwards [41] [42]. The maximum adsorbed quantities of Pb^{2+} ions are 25.32 mg/g with the fine fraction and 34.45 mg/g with the organomodified fine fraction. The quantity adsorbed by the organoclay is greater than that obtained with the fine fraction; which could be explained by the fact that DMSO increases the interlayer distance of kaolinite and therefore promotes adsorption [20].

3.8. Modeling of the Adsorption Isotherm

The authors have adopted the classic models of Langmuir and Freundlich adsorption isotherms, which allow by linear regression to obtain the values of the constants (Q_{max}, K_L, $1/n$ and K_F) in order to better interpret the adsorption results obtained.

a) Langmuir model

Figure 11 and **Figure 12** give the Langmuir model obtained respectively from the fine fraction and the organomodified clay. This model is obtained by drawing the line:

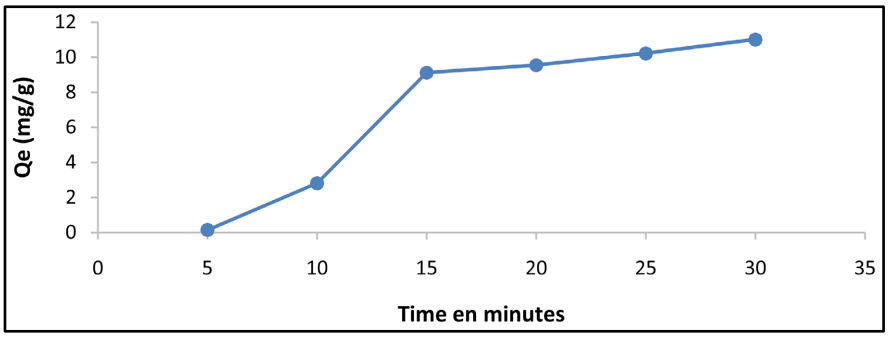

Figure 8. Quantity adsorbed as a function of contact time.

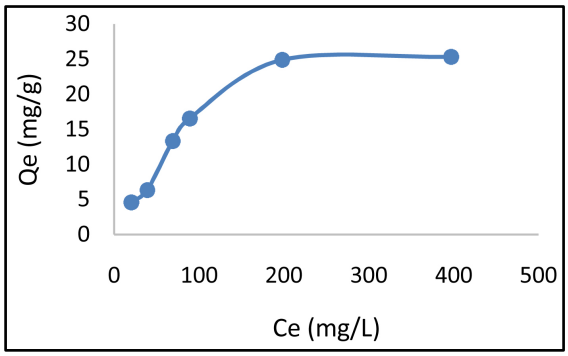

Figure 9. Adsorption isotherm of the fine fraction.

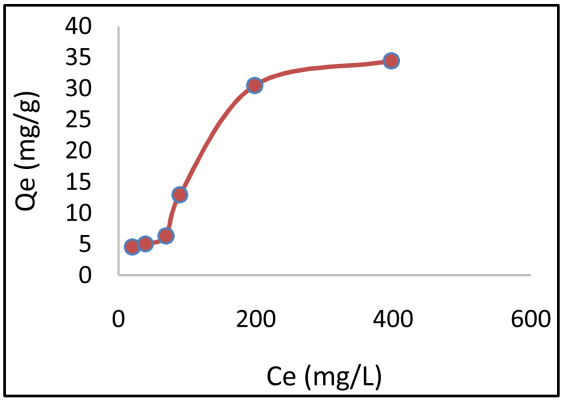

Figure 10. Adsorption isotherm of the intercaleted clay.

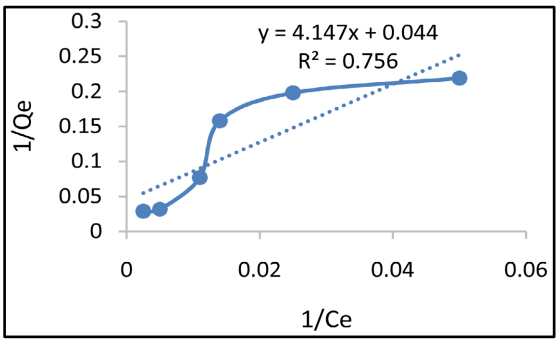

Figure 11. Langmuir model on Pb^{2+} by crude fine fraction.

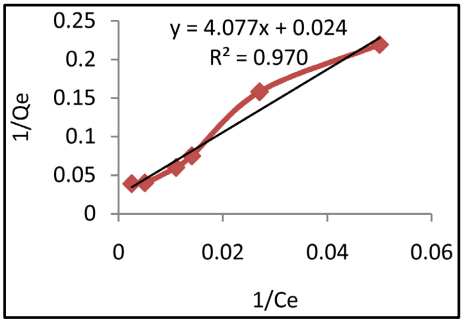

Figure 12. Langmuir model on Pb^{2+} by organomodifiedclay.

$$\frac{1}{Q_e} = \frac{1}{Q_{\max} \cdot K_L \cdot C_e} + \frac{1}{Q_{\max}} \tag{3}$$

with:

$Q_{\max}$: monolayer capacity of the adsorbent (mg/g)

K_L : Langmuir adsorption constant

$\frac{1}{Q_{\max}}$: origin coordinate

$\frac{1}{Q_{\max} \cdot K_L}$ slope

The linearization of the Langmuir equations made it possible to determine the parameters grouped in Table 1.

The parameter $Q_{\max}$ (mg/g) which expresses the maximum adsorption capacity of the monolayer of the material is 22.471 mg/g for the fine fraction and 41.493 mg/g for the organomodified clay. This high maximum quantity in the organomodified clay would confirm the success of the intercalation of DMSO in this clay. The K_L coefficient, which is the equilibrium constant, is equal to 1.07×10^{-2} L/mg for the fine fraction and 5.9×10^{-3} L/mg for the organomodified clay. These values being low would induce a fairly strong adsorption of lead particles by the two matrices [43].

b) Freundlich model

Figure 13 and Figure 14 present the Freundlich model obtained from the fine fraction and the organomodified clay by drawing the straight line:

$$\ln Q_e = \ln K_F + \frac{1}{n} \ln C_e \tag{4}$$

The linearization of the Freundlich equations made it possible to determine the parameters grouped together in Table 2.

K_F and $1/n$ are Freundlich constants related to the temperature, the nature of the adsorbate and the adsorbent. In both cases, the determined K_F coefficient is the same and equal to 4.09 L/mg. It is the same for $1/n$ which is close to 0.62; which would indicate a strong adsorption of Pb^{2+} ions by the studied materials [29].

In view of the values of the coefficients ($Q_{\max}$, K_L, $1/n$ et K_F) obtained, we

Table 1. Lines and linearization coefficients of the Langmuir model.

Adsorbent	Line	Correlation factor (R^2)	Q_{max}	K_L (L/mg)
Fine fraction	$y = 4.147x + 0.0445$	0.7562	22.471	1.07×10^{-2}
Organomodifiedclay	$y = 4.0774x + 0.0241$	0.9701	41.493	5.9×10^{-3}

Table 2. Parameters of the linearization of the Freundlich model.

Adsorbent	Line	Correlation factor (R^2)	$1/n$	K_F (L/mg)
Fine Fraction	$y = 0.6277x - 0.2557$	0.9055	0.6277	4.093
Organomodifiedclay	$y = 0.6233x - 0.2278$	0.9126	0.6233	4.092

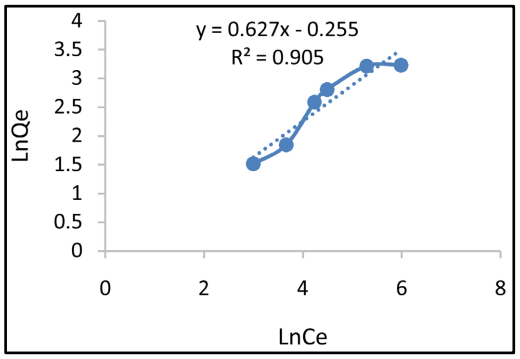

Figure 13. Freundlich model on Pb^{2+} by the crude fine fraction.

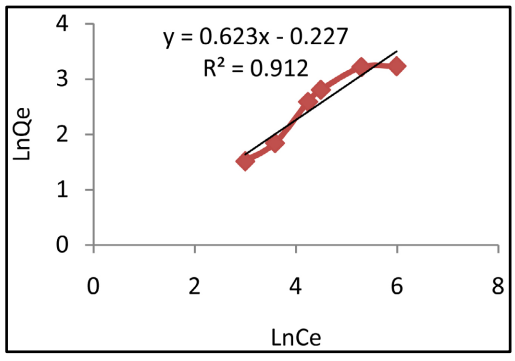

Figure 14. Freundlich model on Pb^{2+} by the organomodifiedclay.

deduce that the Langmuir model may be adequate to model the adsorption isotherm of lead by the clay studied.

4. Conclusion

X-ray diffraction analysis revealed that theMoukosso's soil consists of muscovite (29.7%), kaolinite (8.9%), anatase (2.4%) and quartz (58.9%). Muscovite is the dominant clay species in the Moukosso's soil. The infrared spectrum of the in-

tercalated clay showed, in addition to bands of muscovite (3621 and 1020 cm^{-1}) and kaolinite (3697, 3621, 1020 cm^{-1}), DMSO-specific bands at 1008 and 1070 cm^{-1}. The thermogravimetric analysis showed that the overall mass loss of the organoclay (25%) is greater than that obtained with the raw clay (8.5%), thus confirming the success of the intercalation. The authors observed rapid adsorption of Pb^{2+} ions between 5 and 15 minutes of stirring time in the cases of raw clay and clay intercalated with DMSO. The isotherms obtained are of type S with an adsorption quantity of 22.471 mg/g of the fine fraction and 41.493 mg/g of the intercalated clay. The adsorption of Pb^{2+} ions by the fine fraction and by the organoclay can be interpreted by the Langmuir model.

Conflicts of Interest

The authors declare no conflicts of interest regarding the publication of this paper.

References

[1] Ngoro-Elenga, F., AtipoItouaNgopoh, Elenga, H., Mambou, J.-M., NgakossoNgolo, J.N. and Nsongo, T. (2021) Characterization and Application of the Makoua Clay in the Chemical and Bacteriological Depollution of Gutter and Well Waters of Brazzaville. *Materials Sciences and Applications*, **12**, 263-275. https://doi.org/10.4236/msa.2021.126018

[2] Churchman, G.J., Gates, W.P., Theng, B.K.G. and Yuan, G. (2006) Chapter 11.1 Clays and Clay Minerals for Pollution Control. *Developments in Clay Science*, **1**, 625-675. https://doi.org/10.1016/S1572-4352(05)01020-2

[3] Makhoukhi, B., Villemin, D. and Didi, M.A. (2013) Preparation, Characterization and Thermal Stability of Bentonite Modified with Bis-Imidazolium Salts. *Materials Chemistry and Physics*, **138**, 199-203. https://doi.org/10.1016/j.matchemphys.2012.11.044

[4] Guo, Y.X., Liu, J.H., Gates, W.P. and Zhou, C.H. (2020) Organo-Modification of Montmorillonite. *Clays and Clay Minerals*, **68**, 601-622. https://doi.org/10.1007/s42860-020-00098-2

[5] Lazaratou, C.V., Vayenas, D.V. and Papoulis, D. (2020) The Role of Clays, Clay Minerals and Clay-Based Materials for Nitrate Removal from Water Systems: A Review. *Applied Clay Science*, **185**, Article ID: 105377. https://doi.org/10.1016/j.clay.2019.105377

[6] Kennedy, K.K., Maseka, K.J. and Mbulo, M. (2018) Selected Adsorbents for Removal of Contaminants from Wastewater: Towards Engineering Clay Minerals. *Open Journal of Applied Sciences*, **8**, 355-369. https://doi.org/10.4236/ojapps.2018.88027

[7] El Bastamy, E., Ibrahim, L.A., Ghandour, A., Zelenakova, M., Vranayova, Z. and Abu-Hashim, M. (2021) Efficiency of Natural Clay Mineral Adsorbent Filtration Systems in Wastewater Treatment for Potential Irrigation Purposes. *Sustainability*, **13**, 5738. https://doi.org/10.3390/su13105738

[8] Awasthi, A., Jadhao, P. and Kumari, K. (2019) Clay Nano-Adsorbent: Structures, Applications and Mechanism for Water Treatment. *SN Applied Sciences*, **1**, 1-21. https://doi.org/10.1007/s42452-019-0858-9

[9] Gu, S., Kang, X., Wang, L., Lichtfouse, E. and Wang, C. (2019) Clay mineral Adsor-

bents for Heavy Metal Removal from Wastewater: A Review. *Environmental Chemistry Letters*, **17**, 629-654. https://doi.org/10.1007/s10311-018-0813-9

[10] Undabeytia, T., Shuali, U., Nir, S. and Rubin, B. (2021) Applications of Chemically Modified Clay Minerals and Clays to Water Purification and Slow Release Formulations of Herbicides. *Minerals*, **11**, 1-42. https://doi.org/10.3390/min11010009

[11] Lazorenko, G., Kasprzhitskii, A. and Yavna, V. (2018) Synthesis and Structural Characterization of Betaine and Imidazoline-Based Organoclays. *Chemical Physics Letters*, **692**, 264-270. https://doi.org/10.1016/j.cplett.2017.12.054

[12] Msadok, I., Hamdi, N., Rodríguez, M.A., Ferrari, B. and Srasra, E. (2020) Synthesis and Characterization of Tunisian Organoclay: Application as Viscosifier in Oil Drilling Fluid. *Chemical Engineering Research and Design*, **153**, 427-434. https://doi.org/10.1016/j.cherd.2019.11.010

[13] Díaz, M., Villa-García, M.A., Duarte-Silva, R. and Rendueles, M. (2017) Preparation of Organo-Modified Kaolinite Sorbents: The Effect of Surface Functionalization on Protein Adsorption Performance. *Colloids and Surfaces A*: *Physicochemical and Engineering Aspects*, **530**, 181-190. https://doi.org/10.1016/j.colsurfa.2017.07.067

[14] Olusegun, S.J., De Sousa Lima, L.F. and Mohallem, N.D.S. (2018) Enhancement of Adsorption Capacity of Clay through Spray Drying and Surface Modification Process for Wastewater Treatment. *Chemical Engineering Journal*, **334**, 1719-1728. https://doi.org/10.1016/j.cej.2017.11.084

[15] Awad, A.M., Shaikh, S.M.R., Jalab, R., Gulied, M.H., Nasser, M.S., Benamor, A. and Adham, S. (2019) Adsorption of Organic Pollutants by Natural and Modified Clays: A Comprehensive Review. *Separation and Purification Technology*, **228**, Article ID: 115719. https://doi.org/10.1016/j.seppur.2019.115719

[16] Sánchez-Martín, M.J., Dorado, M.C., Del Hoyo, C. and Rodríguez-Cruz, M.S. (2008) Influence of Clay Mineral Structure and Surfactant Nature on the Adsorption Capacity of Surfactants by Clays. *Journal of Hazardous Materials*, **150**, 115-123. https://doi.org/10.1016/j.jhazmat.2007.04.093

[17] BibilaMafoumba, J.C. (2013) Isotherme d'adsorption des ions Cu^{2+} et Ni^{2+} sur l'argile de Dolisie. Mémoire de Master, Université Marien Ngouabi, Brazzaville, 36 p.

[18] Ngoro-Elenga, F. (2013) Adsorption des ions chromates par l'argile d'Impfondo. Mémoire de Master, Université Marien Ngouabi, Brazzaville, 33 p.

[19] KangouYaba-Ngo, K.J. (2015) Adsorption des ions nickel Ni^{2+} sur quelques argiles prélevées au Congo. Mémoire de CAPES, Université Marien Ngouabi, Brazzaville, 40 p.

[20] Mbaye, A., Diop, C.A.K., Miehe-Brendle, J., Senocq, F. and Maury, F. (2014) Characterization of Natural and Chemically Modified Kaolinite from Mako (Senegal) to Remove Lead from Aqueous Solutions. *Journal of Materials Chemistry*, **49**, 527-539. https://doi.org/10.1180/claymin.2014.049.4.03

[21] Unuabonah, E.I., Kayode, O., Adebowale and Dawodu, F.A. (2008) Equilibrium, Kinetic and Sorber Design Studies on the Adsorption of Aniline Blue Dye by Sodium Tetraborate-Modified Kaolinite Clay Adsorbent. *Journal of Hazardous Materials*, **157**, 397-409. https://doi.org/10.1016/j.jhazmat.2008.01.047

[22] Dejou, J. (1987) La surface spécifique des argiles, sa mesure, relation avec la CEC et son importance agronomique. In: La capacité d'échange cationique et la fertilisation des sols. Amyet Y. édition, 72-83.

[23] Balze, D. (2006) Guide des analyses en pédologie: Choix, expression, présentation, interpretation. Vol. 1, INRA, Paris.

[24] Assifaoui, A. (2002) Etude de la stabilité des barbotines à bases d'argiles locales: Applications aux formulations céramiques industrielles. Doctorat, Université Hassan II, Casablanca, 140 p.

[25] Konan, K.L., Sei, J., Soro, N.S., Oyetola, S., Gaillard, J.-M., Bonnet, J.-P. and Kra, G. (2006) Caractérisation de matériaux argileux du site d'Azaguie-Blida (Anyama, Cote d'Ivoire) et détermination des propriétés mécaniques des produits céramiques. *Journal de la Société Ouest-Africaine de Chimie*, **21**, 35-43.

[26] Bergaya, F., Theng, B.K.G. and Lagaly, G. (2006) Handbook of Clay Science. Vol. 1, Elsevier, Amsterdam, 1248 p. https://doi.org/10.1016/S1572-4352(05)01001-9

[27] Koffi, L.K. (2006) Interaction entre des matériaux argileux et un milieu basique riche en calcium. Thèse de Doctorat, Université de Limoges, Limoges, 144 p.

[28] Zhen, R., Jiang, S.Y., Li, F.F. and Xue, B. (2016) A Study on the Intercalation and Exfoliation of Illite. *Research on Chemical Intermediates*, **43**, 679-692. https://doi.org/10.1007/s11164-016-2645-1

[29] Farmer, V.C. (1974) The Infrared Spectra of Minerals. Mineralogical Society, London, 539. https://doi.org/10.1180/mono-4

[30] Prost, R., Damene, A., Huard, E., Driard, J. and Leydecker, J.P. (1989) Infrared Study of Structural OH in Kaolinite, Dickite, Nacrite and Poorly Crystalline Kaolinite at 5 to 600K. *Clay and Clay Minerals*, **37**, 464-468. https://doi.org/10.1346/CCMN.1989.0370511

[31] Moutou, J.M., Mbedi, R., Elimbi, A., Njopwouo, D., Yvon, J., Odile Barres and Ntekela, H.R. (2012) Mineralogy and Thermal Behaviour of the Kaolinitic Clay of Loutété (Congo-Brazzaville). *Research Journal of Environmental and Earth Sciences*, **4**, 316-324.

[32] Wilson, M.J. (1996) Clay Mineralogy: Spectroscopy and Chemical Determinative Methods. Chapman and Hall, London, 367.

[33] Voula, R., Diamouangana, F., Moutou, J., Samba, V., Foutou, M. and Ngoma, J. (2021) Characterization and Valuation of a Clay Soil Sampled in Londéla-Kayes in the Republic of Congo. *Journal of Minerals and Materials Characterization and Engineering*, **9**, 117-133. https://doi.org/10.4236/jmmce.2021.92009

[34] Ndjioumou, C. (2007) Caractérisations et utilisation des argiles dans l'élaboration des minéraux réfractaires. Université de Yaoundé I, Youndé (Cameroun), 119 p.

[35] Hajjaji, M., Kacim, S., Alami, A., El Bouadili, A. and El Mountassir, M. (2001) Chemical and Mineralogical Characterization of a Clay Taken from the Moroccan Meseta and a Study of the Interaction between Its Fine Fraction and Methylene Blue. *Applied Clay Science*, **20**, 1-12. https://doi.org/10.1016/S0169-1317(00)00041-7

[36] Abidallah, F. (2008) Préparations et caractérisations des nanocomposites polystyrène kaolin. Mémoire de Magister. Université des Sciences et de la Technologie d'Oran, Algérie, 64 p.

[37] Zheng, Q., Zhang, Y., Liu, T., Huang, J. and Xue, N. (2018) Removal Process Structural Oxygen from Tetrahedrons in Muscovite during Acid Leaching of Vanadium-Bearing Shale. *Minerals*, **8**, 208. https://doi.org/10.3390/min8050208

[38] Benredouane, A.D., Kacimi, L., Largo, R.O. and Lopez Delargo, A. (2014) Elaboration d'une pouzzolane artificielle à base de la Zéolithe X synthétisée à partir du kaolin naturel. *MATEC Web of Conference*, **11**, Article No. 01005. https://doi.org/10.1051/matecconf/20141101005

[39] Moutou, J.M., BibilaMafoumba, C., Matini, L., Ngoro-Elenga, F. and Kouhounina,

L. (2018) Characterization and Evaluation of the Adsorption Capacity of Dichromate Ions by a Clay Soil of Impfondo. *Research Journal of Chemical Sciences*, **8**, 1-14.

[40] Achour, S. and Youcef, L. (2003) Elimination du cadmium par adsorption sur bentonite sodique et calcique. *Larhyss Journal*, **2**, 68-81.

[41] Nabil, B. (2007) Etude de l'adsorption de micropolluants organiques sur la bentonique. Mémoire de Magister, Université 20 août 55, Algérie, 91 p.

[42] Errais, E. (2011) Réactivité de surface d'argiles naturelles: Etude des colorants anioniques. Thèse de doctorat, Université de Strasbourg, Strasbourg, 210 p.

[43] Belaïdi, I. (2016) Modification de la bentonite par un sel de bisimidazolium et Applications à l'adsorption du Chrome (III) et du Nickel (II). Mémoire de Master, Université Abou Bakr Belkaid-Tlemcen, Algérie, 98 p.